

# Synthesis of Diphenylmethane Using Iron-containing Mesoporous Catalysts Prepared by Sol-gel Method

Wu Panpan<sup>1</sup>, Wang Qing<sup>1</sup>, Tang Huijie<sup>1</sup>, Xu Lingliang<sup>1</sup>, Jin Hongxiao<sup>1</sup>,  
Ge Hongliang<sup>1</sup>, Wang Xinqing<sup>1</sup>, Lou Hui<sup>2</sup>, Jin Dingfeng<sup>1,2</sup>, Guo Huijun<sup>2</sup>

<sup>1</sup> China Jiliang University, Hangzhou 310018, China; <sup>2</sup> Zhejiang University, Hangzhou 310028, China

**Abstract:** Using sol-gel method, the iron-containing nanocomposites with the ferric citrate as iron source were synthesized. The clear sols were gelled at room temperature and then treated at 60 °C in vacuum to get dry gels which were characterized by thermogravimetric analysis (TG). Finally, mesoporous Fe<sub>2</sub>O<sub>3</sub>/SiO<sub>2</sub> nanoparticles were obtained by the calciner at 400 °C for 3 h. The structure and properties of synthesized particles were investigated by X-ray diffraction (XRD), N<sub>2</sub> adsorption-desorption technique, transmission electron microscopy (TEM), Fourier-transform IR spectroscopy (FT-IR), and temperature programmed reduction (H<sub>2</sub>-TPR). Results reveal that the iron active centers are incorporated into the silica framework with spherical particles size about 50 nm and an average pore diameter of 3.0~4.5 nm. The catalytic activity of nanocatalysts was tested in the synthesized diphenylmethane by Friedel-Crafts alkylation reaction. Results show that the catalysts exhibit an excellent activity with 100% conversion of benzyl chloride and relatively higher selectivity to diphenylmethane, and could be reused multiple times.

**Key words:** sol-gel; Fe<sub>2</sub>O<sub>3</sub>; catalysts; diphenylmethane; Friedel-Crafts; benzyl chloride

Friedel-Crafts alkylations are the very significant category of organic reactions<sup>[1,2]</sup>. One of the most important productions composed by Friedel-Crafts benzylation of benzene with benzyl chloride (BC) is diphenylmethane (DPM), which is commonly used as pharmaceutical intermediates and fine chemicals in the medicine, perfume, pesticide or dye industry<sup>[3-5]</sup>. However, the traditional homogeneous Lewis acid and protonic acid catalysts generally applied for such reactions are highly toxic, corrosive, and difficult to separate and reuse<sup>[4-7]</sup>. Hence, it is highly desirable to replace these catalysts by heterogeneous solid catalysts which are reproducible and friendly to environment, and much work has been focused on the synthesis, properties and applications of heterogeneous catalysts<sup>[8-12]</sup>.

Fe-containing nano-mesoporous materials, such as Fe-M-Mor<sup>[5]</sup>, Fe-MCM-41<sup>[13]</sup>, Fe-ZSM-5<sup>[14]</sup>, Fe-KIT-5<sup>[15]</sup>, Fe-PS-1<sup>[16]</sup>, Fe-FDU-5<sup>[17]</sup>, have been used in a wide range for the synthesis of DPM via benzene and BC. Particularly, Fe<sub>2</sub>O<sub>3</sub>/SiO<sub>2</sub> nanocomposites have been of considerable interest because of their excellent catalytic behavior<sup>[18,19]</sup>. Silica shell is nontoxic and chemically inert and makes no effect on the redox reaction without blocking the pores<sup>[20,21]</sup>. Meanwhile, the shell-core structure prevents coagulation and forms highly

separated redox center. So the mesoporous catalyst exhibits outstanding catalytic activity due to its isolated Fe<sup>3+</sup> active sites on the silica framework and the Fe<sub>2</sub>O<sub>3</sub> nanoclusters in the channel<sup>[5, 14, 22]</sup>. Sol-gel method is one of the frequently-used approaches to synthesize Fe-Si compound materials. Through this method, Fe<sub>2</sub>O<sub>3</sub>/SiO<sub>2</sub> nanoparticles with high porosity, high specific surface area, and highly uniform particle size and morphology can be prepared<sup>[23-26]</sup>. Whereas, it is well-known that Fe<sub>2</sub>O<sub>3</sub> phase obtained by sol-gel method is often affected by a wide range of experiment conditions, including nature of solvents (water, ethanol, etc), the chemical composition and ratios of the precursors, and temperature of gelatin and thermal treatment, etc<sup>[27-30]</sup>.

In this work, Fe<sub>2</sub>O<sub>3</sub>/SiO<sub>2</sub> mesoporous nanoparticles with different Si/Fe ratios were synthesized via sol-gel method. We compared their structural characterizations and discussed their catalytic performance in the benzylation of benzene with benzyl chloride.

## 1 Experiment

### 1.1 Preparation of catalysts

The following chemicals were analytical reagents, and were

Received date: July 25, 2017

Foundation item: National Natural Science Foundation of China (21103154); Zhejiang Provincial Natural Science Foundation of China (LY16B030006)

Corresponding author: Jin Dingfeng, Ph. D., Associate Professor, College of Materials Science and Engineering, China Jiliang University, Hangzhou 310018, P. R. China, Tel: 0086-571-86875610, E-mail: dfjin@cjlu.edu.cn

used without further purification: citric acid ( $C_6H_8O_7 \cdot H_2O$ , 99.5%), ferric citrate ( $C_6H_5O_7Fe \cdot xH_2O$ , Fe 16.5~18.5%), ethyl orthosilicate (TEOS,  $C_8H_{10}O_4Si$ , 98%), ethanol ( $C_2H_5OH$ , 99.7%), benzene ( $C_6H_6$ , 99.5%), benzyl chloride ( $C_7H_7Cl$ , 99.5%).

The synthesis procedure of  $Fe_2O_3/SiO_2$  nanocomposites with different  $n_{Si}/n_{Fe}$  ratios is as follows. 4 g of ferric citrate and 6 g of citric acid (adjust pH value) were dissolved in 20 mL  $H_2O$  by constantly stirring for 6.5 h at 60 °C. The above solution was then added dropwise into 40 mL mixture of TEOS and ethanol to obtain clear sols and gels via continued stirring at room temperature. Finally, the dry gels treated by vacuum at 60 °C, were calcined at 400 °C in air for 3 h. The resultant  $Fe_2O_3/SiO_2$  samples were named as A~E (Table 1).

### 1.2 Characterization of catalysts

The pyrolysis process of the dry gels was characterized by Thermogravimetric Analysis instruments (SDT Q600, TA USA) with a heating rate of 5 °C/min in air. The crystal structure of samples was analyzed by Powder X-ray diffraction (XRD, DX-2700, Dandong Haoyuan Instrument Co., LTD China) with Cu K $\alpha$  radiation at 40 kV and 30 mA.  $N_2$  adsorption-desorption isotherms were measured using a Micromeritics (ASAP 2020, USA). The specific surface areas were obtained using the Brunauer-Emmett-Teller (BET) method, whereas the pore volumes and pore size distributions were estimated from the desorption branches of isotherms using the Barrett-Joyner-Halenda (BJH) model. The morphology of the catalysts was investigated via Transmission Electron Microscopy (TEM, JM-2100, Japan) operated at 200 kV. The Fourier-transform infrared (FTIR) spectra of Fe-Si materials was obtained by the spectrometer (Tensor 27, Bruker Germany) in the range of 400~2000  $cm^{-1}$ . Hydrogen temperature programmed reduction ( $H_2$ -TPR) spectra were recorded on Catalyst Analyzer (BELCAT-B, Japan) equipped with a Thermal Conductivity Detector (TCD).

### 1.3 Catalytic property of catalysts

Friedel-Crafts benzylation of benzene reaction with benzyl chloride to synthesize diphenylmethane was chosen to evaluate the catalytic activity of  $Fe_2O_3/SiO_2$  samples. The reactions were totally performed in a 100 mL three-necked round-bottomed flask, which was equipped with a reflux condenser and heated in a precisely controlled oil bath in the magnetically stirred mode. In a typical process, 30 mL benzene and a certain amount of catalysts were added into the flask and stirred at 50 °C for 10 min at a moderate speed, and then 3 mL BC was added by drop and

all the reaction mixtures were heated to 75 °C and kept for several hours under vigorously stirring. After cooling to room temperature, the liquid samples were withdrawn and analyzed by a FID gas chromatography (GC-1690). The solid catalysts were separated by filtering, washed by ethanol and then calcined at 400 °C for 3 h to reuse.

## 2 Results and Discussion

### 2.1 Structure characterization of catalysts

TG curves of the dry gels with different  $n_{Si}/n_{Fe}$  ratios are shown in Fig.1, which show an obvious three-step mass loss. The first slight slope occurs before 100 °C because of the loss of the adsorbed water. The second sharp slope of the mass loss appears from about 150 °C to 230 °C mainly for the thermolysis of ferric citrate. Finally, the third steep slope of the mass loss from 230 °C to 400 °C indicates the formation of the iron oxide. All dry gels were calcined at 400 °C to obtain  $Fe_2O_3/SiO_2$  nanocomposites according to the results of TG. XRD patterns of the samples with different TEOS contents are presented in Fig.2. It only presents a peak in the  $2\theta$  region of 15~30°, which belongs to amorphous silica phase, and the slightly incisive silica peak changes into broad accompanying the added iron. And no other phases, especially the characteristic reflection peaks of  $Fe_2O_3$  are observed in all the patterns, which indicates the introduced iron is highly dispersed in  $SiO_2$  matrix.

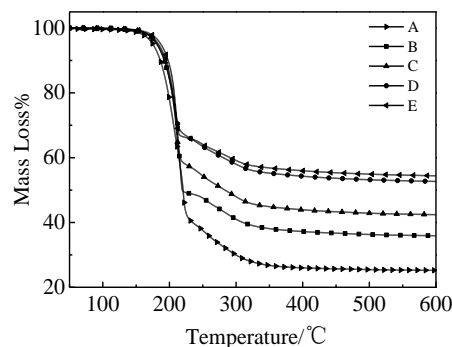


Fig.1 TG curves of dry gels with different  $n_{Si}/n_{Fe}$  ratios

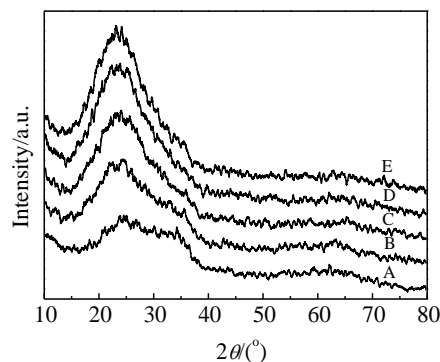


Fig.2 XRD patterns of  $Fe_2O_3/SiO_2$  samples with different TEOS

Table 1 Textural parameters of catalysts with different  $n_{Si}/n_{Fe}$  ratios

Sample	$n_{Si}/n_{Fe}$	$S_{BET}/m^2 g^{-1}$	$V_p/cm^3 g^{-1}$	$D_{BJH}/nm$
A	3	350.87	0.44	4.281
B	5	608.75	0.66	4.329
C	8	768.43	0.70	3.442
D	10	719.79	0.65	3.188
E	13	657.76	0.56	3.070

contents

Fig.3 shows  $N_2$  adsorption-desorption isotherms and BJH pore size distributions of Fe-Si composite materials and the corresponding textural parameters are summarized in Table 1. All the samples display a type IV isotherm with a sharp capillary condensation steep and H1-type hysteresis loop at a relative pressure of 0.45~0.85, which is associated with the presence of mesoporous structure. The height of capillary condensation step increases and hysteresis loop becomes broad with decreasing  $n_{Si}/n_{Fe}$  ratio from 13 to 8, suggesting that iron incorporation helps to improve the texture. The significant increase of the specific surface area, pore volume of catalysts confirms the conclusion. However, all the textural parameters, except for the pore size, decrease upon the continually increased iron contents. This can be interpreted that the composites contain iron species which are linked with the silica framework to destroy the mesoporous structure or which stay inside the nanochannels as the oxide forms to occupy the pore surface<sup>[22, 31]</sup>. Along with decreasing  $n_{Si}/n_{Fe}$  ratio, the pore diameter obviously increases but the pore size distribution turns a uniform and narrow range into a wide. It indicates that the incorporated iron species enhancing the channels and simultaneously disrupting the framework lead to the inhomogeneous particles, which is in close agreement with the XRD patterns of  $SiO_2$ . The morphology of the  $Fe_2O_3/SiO_2$  nanocomposites which were characterized by TEM is shown in Fig.4. The particles fabricated by sol-gel method have nearly spherical morphology and the average particle size is about 50 nm. Nanopores of less than 5 nm are randomly distributed inside of  $Fe_2O_3/SiO_2$  nanoparticles, which is in agreement with the

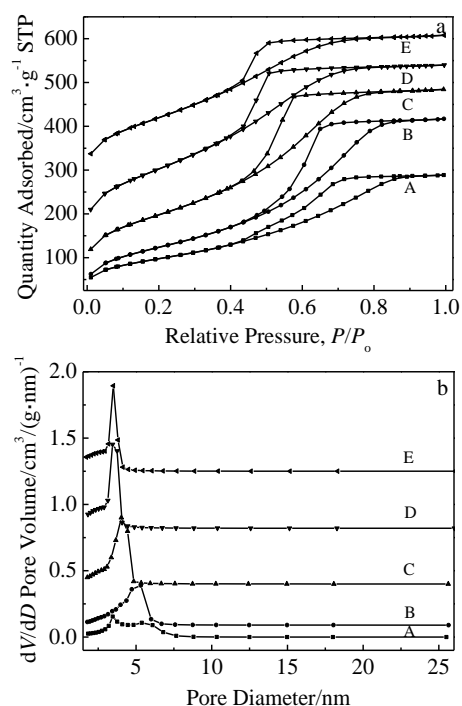


Fig.3  $N_2$  adsorption-desorption isotherms (a) and BJH pore size distribution (b) of Fe-Si composite materials results of the  $N_2$  adsorption isotherm.

FT-IR analysis is used to measure the presence of chemical bonds in the materials and the spectra of prepared samples A to E are shown in Fig.5. The absorption bands at around 800 and 1100  $cm^{-1}$  are attributed to the bending vibrations of Si-O and Si-O-Si stretching vibrations, which verify the formation of the silica shell<sup>[21, 30]</sup>. While the low frequency peaks at about 460  $cm^{-1}$  are assigned to the bending vibrations of Fe-O groups from  $Fe_2O_3$ , whose transmittance intensity weakens with the increasing of TEOS in initial solution<sup>[29]</sup>. Meanwhile, temperature programmed reduction of all the catalysts demonstrates a significant uptake of  $H_2$  as shown in Fig.5. The reduction profile observed at 300~500 °C is identified as the reduction of octahedral coordinated iron species<sup>[17]</sup>, and it increases and shifts to the higher temperature with the increasing Fe contents due to the strong bond-force between incorporated irons and silica supporter.

## 2.2 Catalytic activity

To evaluate the catalytic activity of  $Fe_2O_3/SiO_2$  samples with different Si/Fe ratios, the Friedel-Crafts benzoylation of benzene with BC was investigated as a probe reaction. All the reactions were carried out under the conditions of  $n_{benzene/BC}$  volume ratio of 10 and 0.5 g of catalysts at 75 °C for 1 h to ensure the maximum of reaction and the results are listed in Table 2. Among the Fe-Si catalysts studied, it can be found that all the samples achieve 100% conversion of BC within 1 h. It also shows that the selectivity of DPM is higher than 89% and increases to 95% with decreasing the ratio of  $n_{Si}/n_{Fe}$  from 13 to 8. However, the selectivity decreases along with continually increasing relative

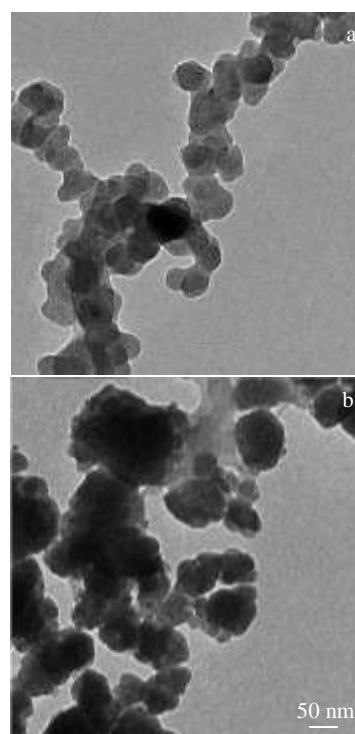


Fig.4 TEM images of the  $\text{Fe}_2\text{O}_3/\text{SiO}_2$  nanocomposites contents of iron since a lot of Fe species block or collapse the nanochannels.

The catalytic performance of sample C according to the reaction time is shown in Fig.6. This catalyst has a very short reaction induction period and rapidly reaches complete BC conversion. The selectivity of DPM is also more than 94% within 15 min with a slight reduction after 50 min because of the formation of few accessory products. Compared to other reported catalysts, such as Fe-Mor<sup>[5]</sup>, and 2.5-FeZ<sup>[14]</sup>, our samples still present higher BC conversion and DPM selectivity and much shorter reaction time, which contributes to not only the highly dispersed iron active sites, but also the enhanced pore channels leading to sufficient accessibility of the active centers to the reactants and the successful diffusion of resultants. Furthermore, the catalyst C is recovered via washing thoroughly by ethanol, drying at 100 °C overnight and calcining again at 400 °C for 3 h, and tested for the next three runs. There is no significant loss in the catalytic performances with nearly 100% conversion and more than 90% selectivity even after three time cycles.

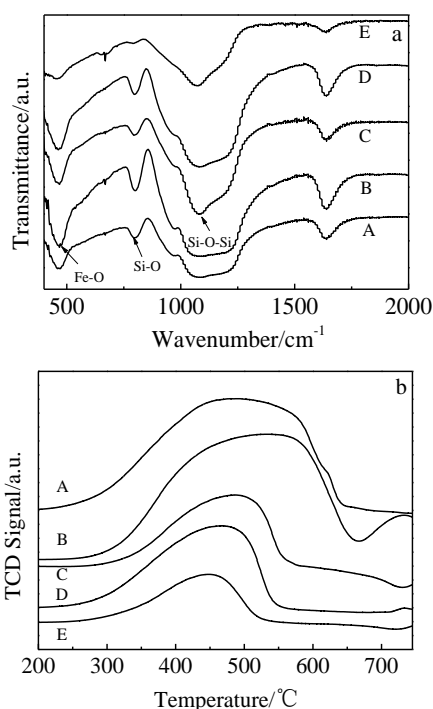


Fig.5 FTIR spectra (a) and TPR curves (b) of catalysts with different  $n_{\text{Si}}/n_{\text{Fe}}$  ratios

**Table 2 Benzylation of benzene with benzyl chloride using different catalysts**

Catalyst	Time/min	BC conversion/%	DPM selectivity/%
A	60	100	90
B	60	100	94
C	60	100	95
D	60	100	92

E 60 100 89  
Conditions: benzene = 30 mL, BC = 3 mL, temperature = 75 °C

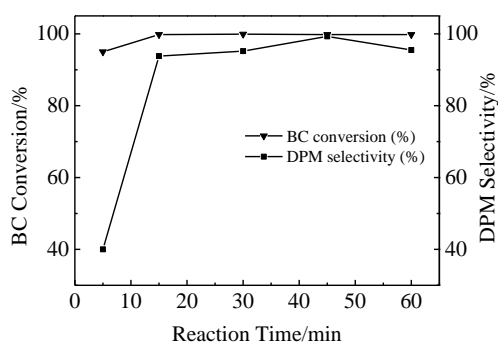


Fig.6 Conversion of BC and selectivity of DPM with different reaction time at 75 °C ( $V_{\text{benzene}}/V_{\text{BC}}=10:1$ , 0.5 g catalyst)

### 3 Conclusions

- 1) Fe-incorporated mesostructure composites, nano- $\text{Fe}_2\text{O}_3/\text{SiO}_2$  has been successfully synthesized via sol-gel method.
- 2) By the XRD,  $\text{N}_2$  adsorption-desorption and  $\text{H}_2$ -TPR techniques, the existence of highly dispersed framework  $\text{Fe}^{3+}$  species is confirmed, and the presence of oxide without aggregation is evidenced via  $\text{N}_2$  adsorption-desorption, TEM and FT-IR measurements.
- 3)  $\text{Fe}_2\text{O}_3/\text{SiO}_2$  nanoparticles possess excellent catalytic performance in the synthesis of DPM by the benzylation of benzene with benzyl chloride. A complete conversion of BC and more than 94% selectivity of DPM are obtained within 15 min over samples C. Moreover, the catalyst can be reused several times without significant loss of the catalytic activity.

### References

- 1 Olah G A. *Friedel-Crafts Chemistry*[M]. New York: Wiley, 1973
- 2 Ahmed A E, Adam F. *Microporous and Mesoporous Materials* [J], 2009, 118: 35
- 3 Candu N, Florea M, Coman S M et al. *Applied Catalysis A: General* [J], 2011, 393(1): 206
- 4 Nguyen D C, Nguyen D H, Tran T H et al. *Journal of Alloys and Compounds*[J], 2014, 582: 83
- 5 Leng Kunyue, Sun Shengnan, Wang Binteng et al. *Catalysis Communications*[J], 2012, 28(44): 64
- 6 Hu X C, Chuah G K, Jaenicke S. *Microporous and Mesoporous Materials*[J], 2002, 53(1): 153
- 7 Leng Kunyue, Wang Yi, Hou Changmin et al. *Journal of Catalysis*[J], 2013, 306(3): 100
- 8 Choudhary V R, Jana S K. *Journal of Molecular Catalysis A: Chemical* [J], 2002,180(1-2): 267
- 9 Bachari K, Cherifi O. *Journal of Molecular Catalysis A: Chemical*[J], 2006, 260(1-2): 19
- 10 Choudhary V R, Jana S K, Patil N S et al. *Microporous and Mesoporous Materials*[J], 2003, 57(1): 21

- 11 Sun Y, Walspurger S, Tessonnier J P et al. *Applied Catalysis A: General*[J], 2006, 300(1): 1
- 12 Jin D F, Wu P P, Zhang M et al. *Microporous and Mesoporous Materials* [J], 2016, 233: 109
- 13 Preethi L E M, Revathi S, Sivakumar T et al. *E-Journal of Chemistry* [J], 2008, 5(3): 467
- 14 Lin Tao, Zhang Xin, Li Rong et al. *Chinese Chemical Letters*[J], 2011, 22(6): 639
- 15 Anand C, Priya S V, Lawrence G et al. *Catalysis Today* [J], 2013, 204(15): 125
- 16 Kanchamreddy R R, Mutyala S, Kantam L M et al. *Indian Journal of Chemistry*[J], 2014, 53: 576
- 17 Srinivasan V V, Imran G, Maheswari R. *Materials Chemistry and Physics* [J], 2015, 165: 72
- 18 Samanta S, Giri S, Sastry P U et al. *Industrial & Engineering Chemistry Research*[J], 2003, 42(13): 3012
- 19 Bhaumik A, Samanta S, Mal N K. *Indian Academy of Sciences* [J], 2005, 65(5): 855
- 20 Niznansky D, Rehspringer J L, Drillon M. *IEEE Transactions on Magnetics*[J], 1994, 30(2): 821
- 21 Chae H S, Kim S S, Piao S H et al. *Colloid and Polymer Science* [J], 2016, 294(4): 647
- 22 Gu J L, Dong X, Elangovan S P et al. *Journal of Solid State Chemistry* [J], 2012, 186(2): 208
- 23 Chang C B, Zhang C R, Wang W Y et al. *Rare Metals*[J], 2010, 29(5): 501
- 24 Zhang X J, Ren W Z, Gui H T et al. *Journal Sol-Gel Science and Technology*[J], 2011, 58(1): 232
- 25 Alagiri M, Hamid S B A. *Journal Sol-Gel Science and Technology*[J], 2015, 74(3): 783
- 26 Masthoff I C, Kraken M, Menzel D et al. *Journal Sol-Gel Science and Technology*[J], 2016, 77(3): 553
- 27 Solinas S, Piccaluga G, Morales M P et al. *Acta Materialia*[J], 2001, 49(14): 2805
- 28 Lu Y, Yin Y D, Mayers B T et al. *Nano Letters*[J], 2002, 22(3): 183
- 29 Xu X J, Wang J, Yang C Q et al. *Journal of Alloys and Compounds*[J], 2009, 468(1-2): 414
- 30 Wang C L, Shaw L L. *Journal Sol-Gel Science and Technology* [J], 2014, 72(3): 602
- 31 Zhai Y P, Dou Y Q, Liu X X et al. *Journal of Materials Chemistry*[J], 2009, 19(20): 3292

## 溶胶凝胶法制备含铁介孔催化剂用于二苯甲烷的合成

吴盼盼<sup>1</sup>, 王 晴<sup>1</sup>, 汤惠睫<sup>1</sup>, 许凌亮<sup>1</sup>, 金红晓<sup>1</sup>, 葛洪良<sup>1</sup>, 王新庆<sup>1</sup>, 楼 辉<sup>2</sup>, 金顶峰<sup>1,2</sup>, 郭慧君<sup>2</sup>

(1. 中国计量大学, 浙江 杭州 310018)

(2. 浙江大学, 浙江 杭州 310028)

**摘要:**采用溶胶凝胶法以柠檬酸铁为铁源合成含 Fe 纳米介孔材料。室温下凝胶样品 60 °C 真空干燥后得到的干凝胶采用热重分析(TG)。最终 400 °C 焙烧 3 h 得到介孔 Fe<sub>2</sub>O<sub>3</sub>/SiO<sub>2</sub> 纳米粒子。合成材料的结构和性能采用 XRD、N<sub>2</sub> 吸脱附、TEM、FT-IF、及 H<sub>2</sub>-TPR 测试方法表征, 结果显示合成了尺寸约 50 nm 的带有 3.0~4.5 nm 介孔孔道的球形 Fe<sub>2</sub>O<sub>3</sub>/SiO<sub>2</sub> 纳米粒子, 并且引入了高分散的 Fe<sup>3+</sup>物种。通过傅克烷基化法合成二苯甲烷的反应测试样品催化性能, 实验结果表明该催化剂具有优异的催化性能, 高达 100% 苄基氯的转化率和相对较高的二苯甲烷的选择性, 并且能够重复利用。

**关键词:** 溶胶凝胶法; Fe<sub>2</sub>O<sub>3</sub>; 催化剂; 二苯甲烷; Friedel-Crafts; 苄基氯

作者简介: 吴盼盼, 女, 1990 年生, 硕士, 中国计量大学材料科学与工程学院, 浙江 杭州 310018, E-mail: 809086072@qq.com